Responses to the comments of Reviewer #1:

We would like to thank the anonymous referee for his/her comprehensive review and valuable suggestions. These suggestions help us to present our results more clearly. In response, we have made changes according to the referee's suggestions and replied to all comments point by point. All the page and line number for corrections are referred to the revised manuscript, while the page and line number from original reviews are kept intact.

Main comments:

1. The study discussed methane emissions from different sectors, but how the sector partitioning is done is not described. I'd suggest authors to provide further methodological details.

Response: We appreciate the reviewer for the insightful comments. Actually, the observed total atmospheric CH_4 concentration integrates emission signals from all sectors, making it difficult to distinguish emission information from different source sectors overlapping in a pixel grid (Saunois et al., 2025). Therefore, the emissions derived from inversion are generally the total emissions at the pixel scale. Following Kou et al. (2025), Zhang et al. (2022), and Miller et al. (2019), we partitioned the optimized total emissions based on the prior proportional information of different sectors within the same model grid. However, it is true that errors in the sectoral proportions of the prior inventory introduce uncertainties into the posterior statistics.

We have added following descriptions and discussions in the revised manuscript. See Lines 377-381, Pages 16-17.

"Assimilating total CH_4 observations alone cannot disentangle emissions from different source sectors overlapping in individual grid cells (Saunois et al., 2025). Consequently, we partitioned the inversion results into respective emission sectors based on the monthly prior proportions at the model grid points (Kou et al., 2025; Zhang et al., 2022), though this approach does introduce a certain degree of uncertainty in sectoral

attribution. The sectoral patterns offer insights into the underlying factors influencing China's emission changes. We concentrated on interpreting the emissions from the coal, gas, rice cultivation… …"

2. The authors have applied TROPOMI XCH4 L2 data. An earlier version of the TROPOMI data have shown substantial regional biases over East China, which may cause errors in the inversion. It would be good if the authors can have some discussion or conduct evaluation on this issue, for instance, using TCCON sites in China.

Response: Thanks for your comments. Indeed, the TROPOMI XCH_4 L2 data product used in this study is Version 02.04.00, and we also identified a considerable number of unrealistically low values in the raw data, particularly during summer (Figure R1). To evaluate the data quality, we compared the raw TROPOMI data with observations from two domestic TCCON stations in China (i.e., Hefei Station and Xianghe Station). The results showed that the raw TROPOMI data underestimated the XCH_4 concentration by 13.2 ppb and 7.8 ppb at these two stations, respectively. This magnitude of negative bias is comparable to the global evaluation results based on 12 TCCON stations, which reported a bias range of -8.5 to -15.5 ppb (PRF-CH4, https://sentiwiki.copernicus.eu/web/s5p-products#S5PProducts-L2S5P-Products-L2). Such negative biases, if unaddressed, would inevitably lead to the underestimation of inverted emissions. However, to avoid the impact of such negative biases on the inversion results, we not only excluded pixels with a qa_value below 0.5 but also selected an alternative XCH_4 product (derived from the WFMD algorithm) to conduct cross-validation. Only the data that met both of the aforementioned criteria were used in the final assimilation. Figure R2 displays the time series of the data after final quality control. It can be observed that this data aligns well with TCCON observations, with relatively small overall differences.

We have added following discussions in the revised manuscript. See lines 294-300, Pages 12-13.

"However, we still found many unrealistic low values, especially in summer. These negative biases can inevitably lead to the underestimation of inverted emissions. To further minimize the impact of outliers, … …Only those pixels that were concurrently available in the TROPOMI/WFMD product and met the quality flag requirements were assimilated. Subsequently, the final quality-controlled TROPOMI data demonstrated good consistency with observations from two TCCON stations, namely the Hefei and Xianghe stations (Figure S3)."

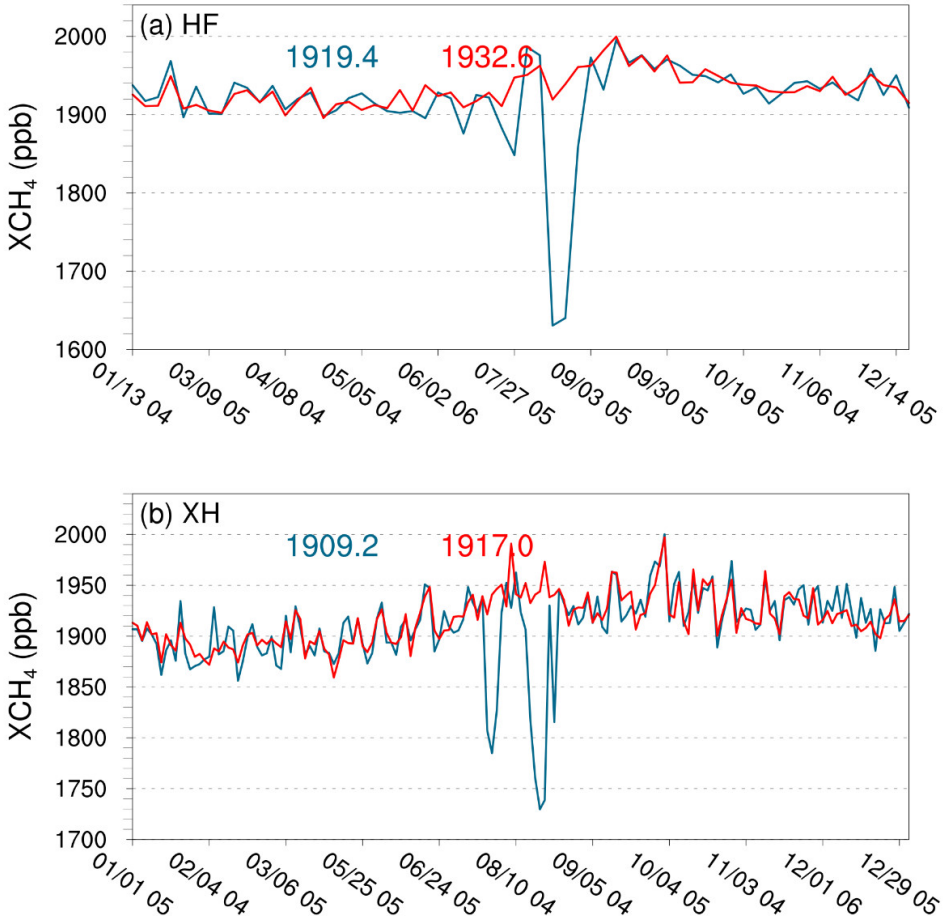

Figure R1 Comparison of time series between operational TROPOMI XCH_4 product filtered by qa_value > 0.5 and TCCON observations at Hefei and Xianghe stations. For the evaluation, only TROPOMI pixels that are located within a 0.1° radius of the respective TCCON station and have a time difference of less than 1 hour relative to TCCON observational records (two spatiotemporal matching criteria) were selected. Specifically, the number of valid matching pairs was 62 for the Hefei station and 163 for the Xianghe station.

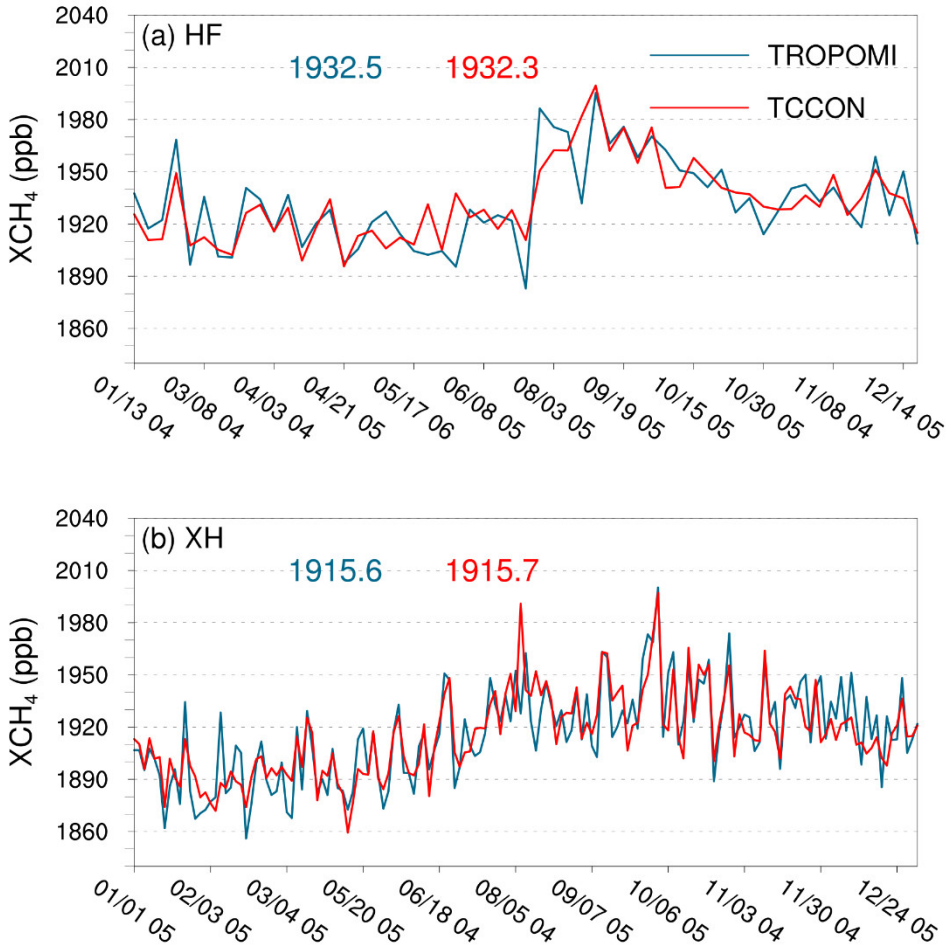

Figure R2 Same as Figure R1, but for the evaluation of TROPOMI data after final quality control. The number of valid matching pairs was 57 for the Hefei station and 155 for the Xianghe station. (Figure S3 in the revised supplementary information)

3. I do appreciate that the authors have performed evaluation for meteorology parameters against independent data, which most of existing studies have not done. This is crucial for characterizing model transport errors and understanding the difference between inversion systems. However, the discussion is overly simple. I'd suggest the authors to expand the results on meteorology evaluation (especially wind). In particular, the evaluation over the D02 domain provides crucial information because of the complex terrain in Shanxi.

Response: We fully agree that CH_4 emission estimates are highly sensitive to biases in meteorological simulations. This is because meteorological processes exert a significant influence on atmospheric transport, which in turn shapes the source-receptor relationships and determines the flow-dependent background error covariance. As shown in Figure R3, we expanded the meteorological evaluation with a specific focus on wind conditions and incorporated an assessment of the meteorological field simulations over Shanxi Province. Overall, across the China domain, the WRF model simulations exhibited biases of -0.4°C for T2, -4.9% for RH2, and 0.5 m/s for WS10. For Shanxi Province, which features complex terrain, the biases were 1.5°C for T2, -12.5% for RH2, and 0.4 m/s for WS10. Notably, the overestimated wind speed in the simulations accelerated the transportation of simulated CH_4 concentrations, which to some extent contributed to the overestimation of inverted CH_4 emissions.

Relevant discussions have been added to the revised manuscript. See Lines 523-537, Pages 22-23.

"CH_4 emission estimates are highly sensitive to biases in meteorological simulations, as meteorological processes significantly influence atmospheric transport, which in turn shapes the source-receptor relationships and determines the flow-dependent background error covariance. Overall, the model demonstrated satisfactory performance in reproducing domain-wide meteorological conditions across China (Figure S6), with minimal biases of -0.4°C for T2 and -4.9% for RH2, alongside high correlation coefficients (CORR) of 1.0 and 0.96, respectively. The model's performance over Shanxi Province was slightly less optimal, likely due to the region's complex terrain. The biases for T2 and RH2 were 1.5°C and -12.5%, respectively, while the CORR remained high at 0.99 and 0.90. Additionally, the WRF model effectively captured the temporal variations in wind direction both across China and Shanxi Province. However, WS10 was generally slightly overestimated, with biases of 0.5 m/s and 0.4 m/s and CORR of 0.88 and 0.81 over China mainland and Shanxi province, respectively. Such overestimation of wind speed in WRF simulations has also been widely reported in other studies (e.g., Hu et al., 2016). An overestimated wind speed

causes the model to simulate faster and more extensive diffusion of CH_4 concentrations than occurs in reality. To compensate for the simulated reduction in CH_4 concentrations due to this excessive diffusion, the inversion system potentially increases the estimated emissions."

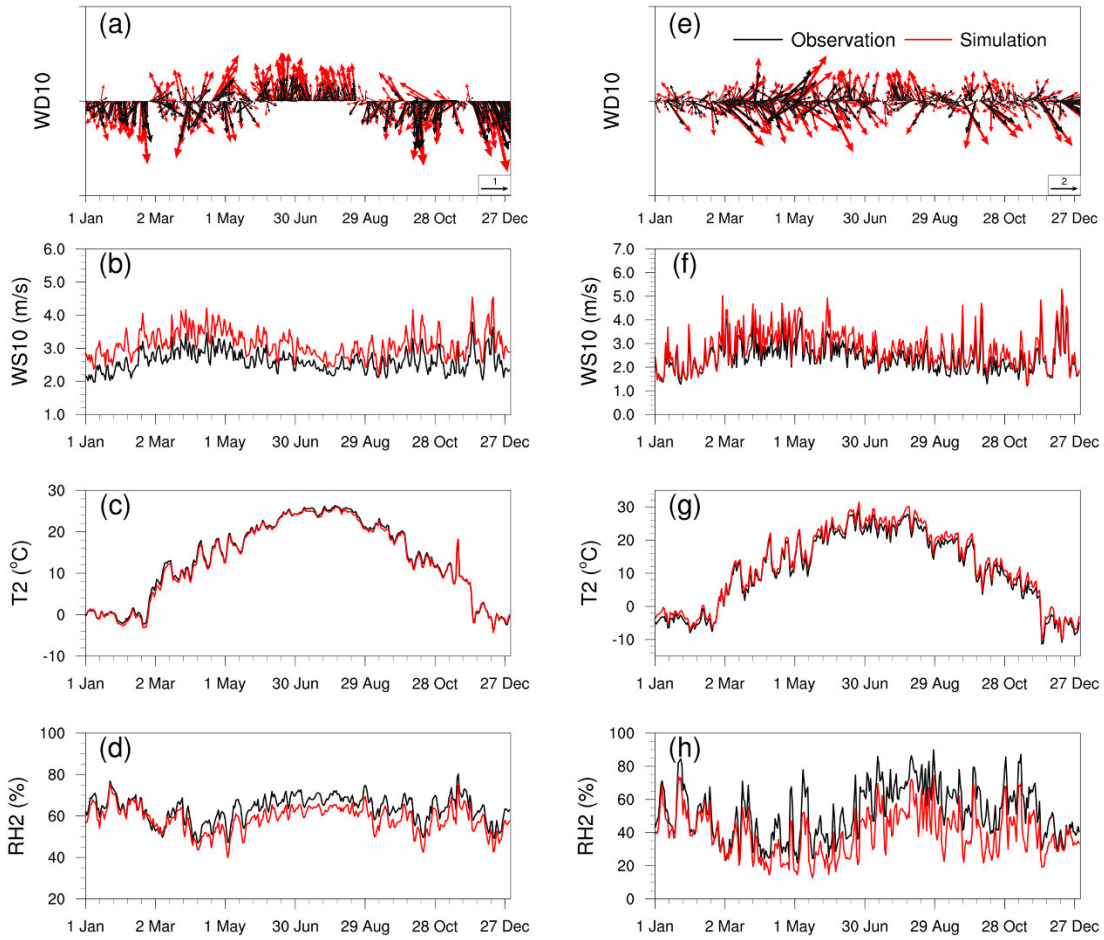

Figure R3 Time series of observed and simulated wind direction at 10 m (WD10), wind speeds at 10 m (WS10, m/s), temperature at 2 m (T2, ℃), and relative humidity at 2 m (RH2, %) across (a-d) China and (e-h) Shanxi Province. China and Shanxi Province include 400 and 26 stations, respectively. (Figure S6 in the revised supplementary information)

4. The authors used the optimized emissions from the D01 inversion as prior emissions for the D02 inversion. This implies that the observations over D02 are used twice in the optimization of emissions. From the Bayesian standpoint, this is

problematic as it leads to over-confidence in observations.

Response: Thanks for this comment. It is important to clarify that in the first inversion window, the prior emissions for both the D01 and D02 domains were derived from the EDGAR inventory. For subsequent inversion windows, the prior emissions (X_b) for D01 and D02 were each obtained from their respective optimized emissions (X_a) in the previous window (Figure R4). Notably, the observational data were used sequentially to optimize the prior emissions of D01 and D02. Specifically, the observations were not reused for the optimization of the same emissions. Instead, D01 only provided a more optimized boundary condition for the emission simulation of D02, rather than serving as the prior emission input for D02.

To enhance clarity on this process, we have added the following description in the revised manuscript. See Lines 152-161, Pages 6-7.

"… …For the same domain, the RegGCAS-CH_4 performed a "two-step" inversion scheme in each data assimilation (DA) window. First, the prior emissions were optimized using the available atmospheric observations. Then, the optimized emissions were input back into the CTM to generate the initial fields for the next assimilation window. Simultaneously, the optimized emissions were transferred to the next window to serve as prior emissions (Figure S1). It is noted that the system optimizes the prior emissions for the D01 and D02 domains separately. Specifically, D01 only provides an optimized boundary field for D02, rather than the prior emission source for D02. Thus, the uncertainties in boundary conditions for D02 emission estimates were reduced. … …"

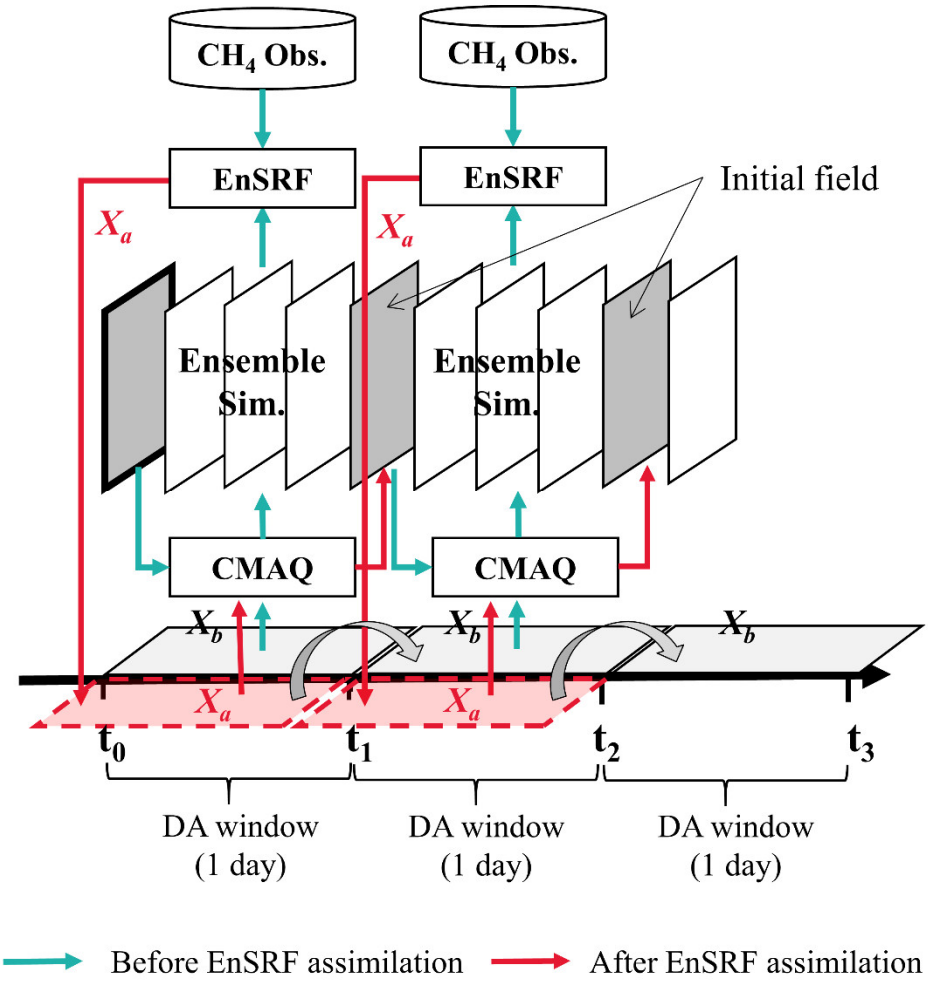

Figure R4 RegGCAS-CH4 assimilation process (Figure S1 in the revised supplementary information)

5. The paper in general lacks uncertainty characterization for emission flux estimates. For regions with limited observation coverage (e.g., Southern China), it is unclear to what degree the posterior estimates depend on prior estimates.

Response: Thank you for this insightful comment. To quantify the overall posterior uncertainty of our emission estimates, we evaluated the combined impacts of multiple influential factors, including the representation of CH_4 chemical processes, boundary conditions, selection of prior inventories, satellite products, and assimilation system parameter settings (Figure R5). Meanwhile, we paid special attention to southern China (a region with limited observation coverage) to assess the degree to which posterior

emissions rely on prior estimates.

Nationwide, adopting the CAMS-GLOB-ANT v6.2 inventory (instead of the base EDGAR inventory) led to a 5.2% increase in posterior emissions. More importantly, the initial difference between the two prior inventories (6.0 Tg) converged to a much smaller difference of 2.3 Tg in the posterior results, indicating good robustness of the assimilation system at the national scale. However, in southern China (south of 30°N), limited observational constraints weakened this convergence. The difference between the two prior inventories (5.8 Tg) only decreased to 4.8 Tg in the posterior emissions, clearly reflecting a higher dependence of posterior estimates on prior information in this region. Using the default CAMS global concentration field (relative to adjusted fields) resulted in a 7.5% increase in posterior emissions; incorporating CH_4 chemical reactions (vs. omitting them) caused a 6.6% increase; assimilating the TROPOMI/WFMD product (vs. the TROPOMI/SRON product) led to a 4.4% increase. In contrast, variations in assimilation system parameters (e.g., observation error, background error, and localization scale) had minimal impacts, restricting changes in posterior emissions to a narrow range of -0.8% to 1.7%. Based on these analyses, we quantified the overall posterior emission uncertainty as 8.5% for mainland China and 7.8% for Shanxi Province.

We have added the above discussion on uncertainty characterization in the revised manuscript.

See Lines 676-736, Pages 31-34.

"… …To better evaluate the potential impact of prior uncertainties on posterior emission estimates, we conducted additional inversion experiments (SENS2) using the 2022 CAMS-GLOB-ANT v6.2 inventory as prior emissions. Nationwide, the posterior emissions in SENS2 increased by 5.2% compared with those in the BASE experiment. More importantly, the initial difference between the two prior inventories (6.0 Tg) converged to a much smaller difference of 2.3 Tg in the posterior results, indicating good robustness of the assimilation system at the national scale. However, in southern

China (south of 30°N), due to limited observational constraints, the difference between the two prior inventories (5.8 Tg) only decreased to 4.8 Tg in the posterior results. In contrast, in observation-dense regions such as Shanxi Province, even though the difference in prior emissions was only 61.9 Gg, the difference in optimized posterior emissions further converged to 39.0 Gg.

Uncertainty in atmospheric transport models can contribute to model-data mismatch errors. Consistent with previous studies (Chen et al., 2022), this study initially omitted CH_4 chemical reactions to accelerate model integration and inversion efficiency. To quantify the impact of this simplification, we further conducted an additional inversion experiment (SENS3) where CH_4 chemical reactions were incorporated into the CMAQ model. Results showed that the inclusion of chemical reactions led to a 6.6% difference compared to the base experiment. Specifically, the difference was small in winter (only 1.7%), whereas in summer, the OH concentration in the lower troposphere was one order of magnitude higher than that in winter (Lelieveld et al., 2016). This stronger OH-driven CH_4 oxidation resulted in an increase of over 10% in posterior emissions. This indicates that accounting for CH_4 chemical reactions in summer is still necessary for accurate emission inversion. The impact of chemical reactions only increased emission estimates by 1.9% in Shanxi Province.

Different satellite products employ distinct inversion algorithms, which in turn determine the quality and quantity of the data. To assess how satellite product selection influences emission inversion, the TROPOMI/WFMD product was assimilated in SENS4. Compared with the operational TROPOMI product in BASE experiment, the TROPOMI/WFMD product provided a 59.3% increase in the number of observations, particularly notable in winter. In mainland China, posterior emissions derived from SENS4 increased by 4.4%, primarily driven by higher emission estimates in March and April. In Shanxi Province, posterior emissions showed a more modest increase of 2.2%.

Our results may also be subject to several uncertainties associated with the settings of assimilation system parameters. In particular, background and observation errors influence the weight assigned to prior emissions versus observations in determining

posterior emissions, while the localization scale dictates the distance over which observational information affects the inversion results. To quantify these impacts, we conducted sensitivity tests by adjusting key parameters: observation errors were set to 0.5% and 0.9% (SENS5-6), background errors to 30% and 50% (SENS7-8), and localization scales to 250 km and 350 km (SENS9-10), respectively. However, our sensitivity analysis revealed that varying these parameters, whether increasing or decreasing their values, only led to differences of -0.7% to 1.7% in posterior emission estimates across mainland China. This indicates that the CH_4 emission estimates were not significantly affected by adjustments to the system parameters.

Following the methods of Feng et al. (2024) and Nassar et al. (2017), we estimated the overall uncertainty of our results by accounting for the combined effects of the aforementioned factors (e.g., parameter settings, prior inventories). In general, sparsely observed regions, such as western China and Northeast China, showed over-reliance on the prior inventory (SENS2) and exhibited relatively high posterior emission uncertainty (28.0–44.1%). In contrast, densely observed regions including East China and North China showed relatively low uncertainty (7.9–17.4%). Across mainland China, boundary condition errors contributed the most to total uncertainty. Specifically, boundary conditions caused substantial differences in emission estimates for Northeast China. The overall posterior emission uncertainty for mainland China was 8.5%, while that for Shanxi Province was even lower at 7.8%, with this uncertainty primarily driven by uncertainties in the prior inventory."

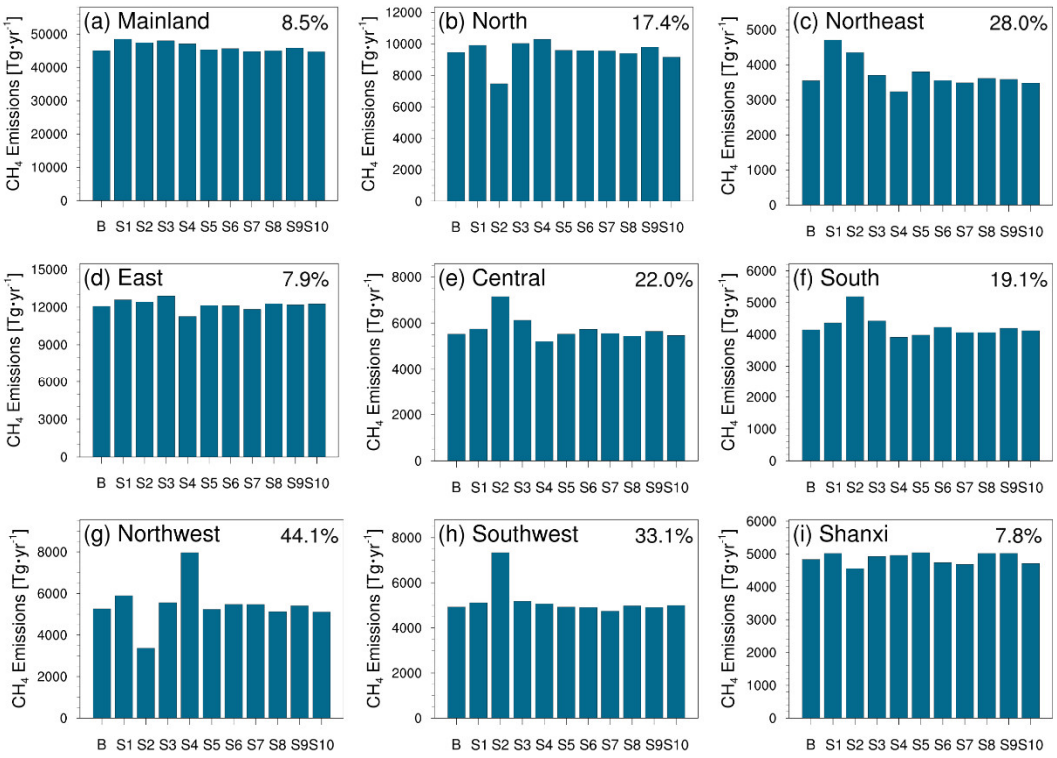

Figure R5 Posterior CH_4 emissions from the base and different sensitivity experiments (Table S6). B denotes the BASE experiment. S1 to S10 denote the SENS1 to SENS10 experiments, respectively. S1 represents the experiment using the unadjusted CAMS global concentration field as the boundary; S2 denotes the experiment adopting CAMS-GLOB-ANT v6.2 inventory as the prior emission inventory; S3 denotes the inversion experiment accounting for CH_4 chemical reactions; S4 denotes the inversion experiment assimilating the TROPOMI/WFMD product; S5 and S6 denote the experiments with observation errors set to 0.5% and 0.9%, respectively; S7 and S8 denote the experiments with background errors set to 30% and 50%, respectively; S9 and S10 denote the experiments with the localization scale adjusted to 250 km and 350 km, respectively. The numbers on the figure represent the uncertainty values of different regions. (Figure 8 in the revised manuscript)

Minor suggestions:

1. L80: key source-> "point source scale" or "local scale"?

Response: We have changed “key source scales” to “local scales”. See Line 80, Page 4.

2. L95: unclear -> uncertain

Response: We have changed “unclear” to “uncertain”. See Line 95, Page 4.

3. L103: To my knowledge, IMI is not an operational inversion system, but more like open-source software. So it may be improper to characterize it as a US system. Similar issues may exist for other listed systems.

Response: Thank you for pointing out this important issue. we have revised the description to accurately reflect its characteristics. See Lines 99-105, Pages 4-5.

“Currently, global-scale CH_4 assimilation systems are widely applied, such as CarbonTracker-CH_4 in the United States (Bruhwiler et al., 2014), CAMS in Europe (Agustí-Panareda et al., 2023), NTFVAR in Japan (Wang et al., 2019), and GONGGA-CH_4 in China (Zhao et al., 2024)… …There are relatively few existing regional CH_4 assimilation systems, such as the ICON-ART-CTDAS (Steiner et al., 2024) and CarbonTracker Europe-CH_4 (Tsuruta et al., 2017) in Europe. Additionally, several open-source frameworks offer inversion tools adaptable to different scales, such as LMDz-SACS-CIF in France (Thanwerdas et al., 2022) and the IMI in the United States (Varon et al., 2022). Nevertheless, most existing regional inversions still rely on global atmospheric transport models with relatively coarse resolutions and… …”

4. L188-189: Any quantitative estimates how much error it will incur for D01 and for D02 respectively, by deactivating the chemical oxidation?

Response: Thank you for this valuable comment. To address your question regarding the quantitative error in CH_4 emission estimates caused by deactivating CH_4 chemical oxidation, we conducted a dedicated sensitivity experiment (SENS3) where full CH_4 chemical reactions were incorporated into the CMAQ model. For the mainland China, the omission of CH_4 chemical reactions results in an overall underestimation of posterior emissions by approximately 6.6% compared to the SENS3 experiment (with reactions activated). For the Shanxi Province, the bias induced by deactivating chemical oxidation is more modest, with an average underestimation of only 1.9% across all seasons. We have supplemented error estimates in the revised manuscript. Please refer to our response to Main Comment 5.

5. L230: How do you specify the R matrix? Also explain specifically that R is an error covariance matrix for what.

Response: We sincerely appreciate your meticulous review. The matrix $\boldsymbol{R}$ is an observation error covariance matrix. It is specified as a diagonal matrix, which assumes that observation errors from different stations at different times are mutually independent (i.e., no covariance between distinct observations). The diagonal elements correspond to the observation errors of the satellite data, set here to be 0.7% (~ 13.3 ppb in mainland China) of the column concentration values. This specification is based on the product's quarterly validation report, which indicates that for the bias-corrected TROPOMI product, the 1σ spread of the relative difference between TROPOMI retrievals and TCCON observations is on the order of 0.7% (Lambert et al., 2025).

We have added a description of the $\boldsymbol{R}$ matrix. See Lines 232-233, Page 10.

"where $\boldsymbol{R}$ is an observation error covariance matrix, which is specified as a diagonal matrix with the assumption that observation errors from different pixels are mutually independent (Feng et al., 2020). $\boldsymbol{K}$ is the Kalman gain matrix … …"

6. L232: Ep: Power plant sources? Seems something copied from a CO2 study.

Response: Thank you for your comment. Indeed, the prior inventory (EDGAR) used in this study includes the "Power Industry" sector (ENE). Given that power plants are typically elevated point sources, they are usually not located in the same model grid as ground-based area sources. This spatial distinction allows for effective separation between these two types of sources. Therefore, even though power plant sources account for a small proportion (0.6%) of total emissions, we treated area sources and power plant sources as separate state vectors for optimization in the inversion process.

We have added additional explanations. See Lines 239-241, Page 11.

"… …industry, transport sources, etc. Given that power plants are typically elevated point sources, this spatial distinction allows for effective separation from ground-based area sources. Therefore, even though power plant sources account for a small proportion (0.6%) of total emissions, we treated them as separate state vectors for optimization. The updated emissions are then… …"

7. L234: No need to capitalize O in oil

Response: The capitalization of "O" in "oil" has been corrected. Thanks. See Line 238, Page 10.

L251: Would 1 day be too short for adequate observation constraint, if you assume that prior errors are independent from one day to the next (L272-273)?

Response: Thank you for this comment. In fact, the prior errors across different inversion windows are not independent, as the prior emissions for each day are derived from the optimized emissions of the previous day. The 40% uncertainty setting is intended to cover the error statistical characteristics of emission variations from one day to the next. This temporal continuity ensures that prior errors do not become completely decoupled between consecutive days.

Theoretically, a longer inversion window would allow CH_4 to undergo more extensive atmospheric transport, enabling more observations to capture the signal of emission changes in a given grid cell. However, as the distance between an observation site and an emission source increases, the emission signal detected by the observation weakens significantly, while noise interference intensifies. Particularly, constrained by the EnKF method with a limited ensemble size, this weakened emission signal tends to be masked by unphysical signals (unrealistic long-distance spurious correlations). Consequently, a longer inversion window does not necessarily yield better performance than a shorter one (Jiang et al., 2021). On the other hand, the TROPOMI satellite provides relatively dense observational data. Even with a short assimilation window (e.g., 1 day), the abundant observations can still effectively capture meaningful emission signals from surrounding grid cells, which is sufficient to optimize regional-scale CH_4 emissions. In contrast, for sparse observational data, a longer assimilation window is typically required to capture emission signals from distant sources.

We have calculated the average number of surrounding observations (all quality-controlled pixels falling into the same grid are averaged into a single observation) that each grid is constrained by per day (Figure R6). Overall, most grids in northern China can be constrained by over 40 observations, while most grids in southern China can be constrained by approximately 10 observations. Additionally, during the assimilation process, we filtered out observations with a correlation coefficient < 0.27 (low significance, with $p > 0.05$) between the emission ensemble and the concentration ensemble at the observation locations. As a result, in the southwest region, some grids are not constrained by observations, accounting for approximately 4.8% of the total grids nationwide; however, the emissions from these unconstrained grids constitute less than 0.0004% of the national total emissions. Therefore, in most parts of the country, a 1-day assimilation window can provide adequate observation constraint.

We have added additional explanations. See Lines 305-309, Page 13.

“For regions with limited observation coverage (e.g., southern China), posterior emission estimates may rely heavily on prior information (see Discussion). On one hand,

the system optimizes emissions in grids surrounding observations through the source-receptor relationship of atmospheric transport, allowing it to impose extensive constraints on emissions (Figure S4); on the other hand, … …"

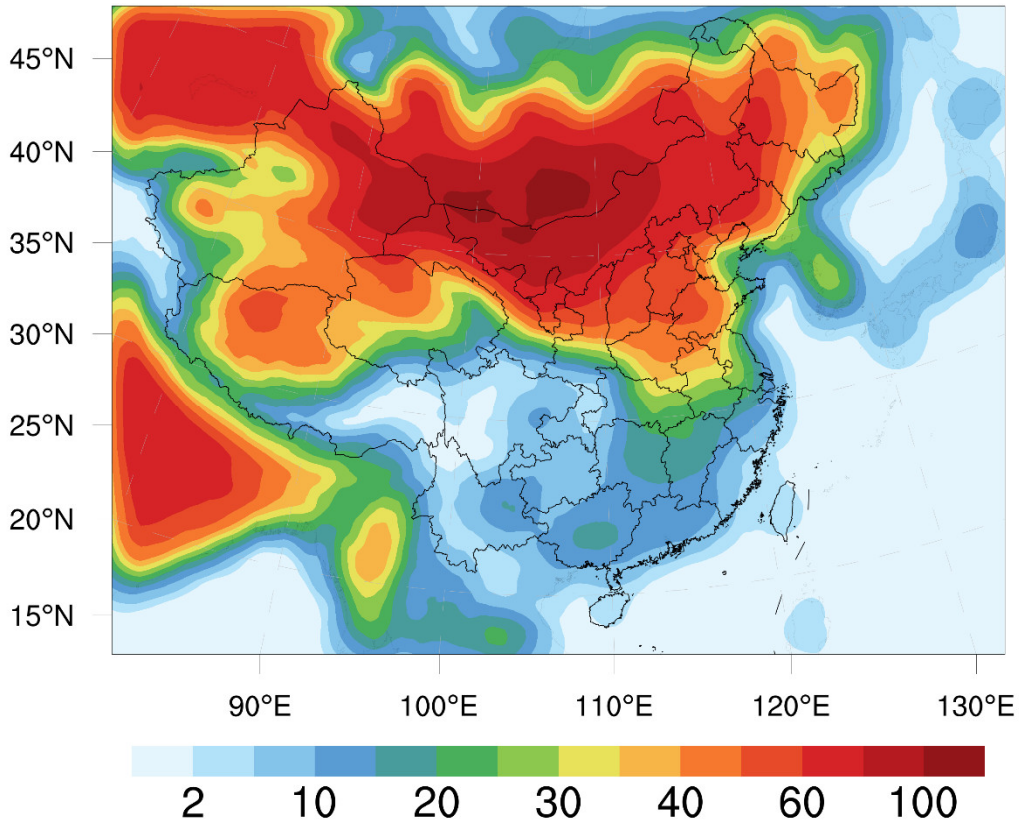

Figure R6 Average number of observations constraining each grid per day. (Figure S4 in the Supplementary Information)

8. Table 1: What do the last two columns (building, mature) stand for?

Response: Thank you for pointing out this ambiguity. "Mature" in the table is a spelling error and should be corrected to "Manure", which corresponds to the "Manure management" sector, a key source of CH_4 emissions from agricultural activities. The "building" represents emissions from small-scale non-industrial stationary combustion, including fuel combustion for heating, cooking, or other energy uses in residential, commercial, or small non-industrial buildings.

We have corrected the typo ("Mature" → "Manure") and added brief annotations for

both columns in the revised Table 1. See Lines 441-443, Page 19

"* Waste includes wastewater treatment, solid waste landfills, and solid waste incineration; Building represents emissions from small-scale non-industrial stationary combustion; Manure refers to emissions from the manure management sector."

9. Table 1 and related discussion (e.g., L360): EDGAR v8.0 is used as prior information. Recent studies have shown that EDGAR has large errors in the spatial and seasonal distribution in rice emissions (Chen et al., 2025; Liang et al., 2024). I'd suggest the authors to briefly discuss the impact on emission quantification and sector attribution in Northeast and East China.

Chen et al.: Global Rice Paddy Inventory (GRPI): a high-resolution inventory of methane emissions from rice agriculture based on Landsat satellite inundation data, Earth's Future, 2025.

Liang et al.: Satellite-based Monitoring of Methane Emissions from China's Rice Hub, Environmental Science & Technology, 2024.

Response: Thank you for this critical comment. We acknowledge that these limitations could potentially affect the accuracy of our prior-based emission quantification and sector attribution, especially for Northeast and East China, dominated by paddy field CH_4 emissions. We have supplemented a discussion of this impact in the revised manuscript.

See Lines 403-412, Pages 17-18.

"Recent studies have highlighted significant errors in the spatial distribution of rice CH_4 emissions in EDGAR v8.0, which relies on outdated rice paddy maps and incorrectly overspreads rice emissions across non-rice agricultural grids (Chen et al., 2025). These limitations not only cause EDGAR to overestimate rice emissions but also lead to overestimation in subsequent posterior emissions. Specifically, this overestimation may inflate the contribution of rice to total CH_4 emissions in posterior attribution, while

simultaneously underestimating the contribution of other CH_4 sources (e.g., coal, wetlands) that coexist in these misclassified grids. Conversely, EDGAR fails to capture recent expansions of rice cultivation in Northeast China, particularly the rapid growth of rice paddies in the Sanjiang Plain (Liang et al., 2024). This omission may result in a systematic underestimation of rice emission hotspots in this region."

See Lines 497-505, Page 21.

"However, EDGAR v8.0 adopts a uniform seasonal profile for rice CH_4 emissions across China, assigning a single emission peak in June to all rice-growing regions. This simplification contradicts the findings of Chen et al. (2025), who reported that rice CH_4 emissions in China generally peak in July–August, with the length of the emission season varying significantly due to the diversity of regional rice cropping systems. Notably, our posterior emission results align well with the seasonal pattern, with the highest monthly rice emissions occurring in August, followed by July (Table S3). This consistency confirms that the TROPOMI satellite observations have effectively corrected the unrealistic uniform seasonal bias inherent in EDGAR."

10. Table 2: Just a comment: The comparison with local observations, which are sensitive to emission adjustment, is valuable.

Response: Thank you very much for your positive comment.

References

Chen, Z., Jacob, D. J., Nesser, H., Sulprizio, M. P., Lorente, A., Varon, D. J., Lu, X., Shen, L., Qu, Z., Penn, E., and Yu, X.: Methane emissions from China: a high-resolution inversion of TROPOMI satellite observations, Atmos. Chem. Phys., 22, 10809-10826, 10.5194/acp-22-10809-2022, 2022.

Chen, Z., Lin, H., Balasus, N., Hardy, A., East, J. D., Zhang, Y., Runkle, B. R. K., Hancock, S. E., Taylor, C. A., Du, X., Sander, B. O., and Jacob, D. J.: Global Rice Paddy Inventory (GRPI): A High-Resolution Inventory of Methane Emissions From Rice Agriculture Based on Landsat Satellite Inundation Data, Earth's Future, 13, e2024EF005479, 10.1029/2024EF005479, 2025.

Hu, J., Chen, J., Ying, Q., and Zhang, H.: One-year simulation of ozone and particulate matter in China using WRF/CMAQ modeling system, Atmos. Chem. Phys., 16, 10333-10350, 10.5194/acp-16-10333-2016, 2016.

Jiang, F., Wang, H., Chen, J. M., Ju, W., Tian, X., Feng, S., Li, G., Chen, Z., Zhang, S., Lu, X., Liu, J., Wang, H., Wang, J., He, W., and Wu, M.: Regional CO2 fluxes from 2010 to 2015 inferred from GOSAT XCO2 retrievals using a new version of the Global Carbon Assimilation System, Atmos. Chem. Phys., 21, 1963-1985, 10.5194/acp-21-1963-2021, 2021.

Kou, X., Peng, Z., Han, X., Li, J., Qin, L., Zhang, M., Parker, R. J., and Boesch, H.: China's methane emissions derived from the inversion of GOSAT observations with a CMAQ and EnKS-based regional data assimilation system, Atmospheric Pollution Research, 16, 102333, 10.1016/j.apr.2024.102333, 2025.

Lambert, J.-C., A. Keppens, S. Compernolle, K.-U. Eichmann, M. de Graaf, D. Hubert, B. Langerock, M.K. Sha, E. van der Plas, T. Verhoelst, T. Wagner, C. Ahn, A. Argyrouli, D. Balis, K.L. Chan, M. Coldewey-Egbers, I. De Smedt, H. Eskes, A.M. Fjæraa, K. Garane, J.F. Gleason, J. Granville, P. Hedelt, K.-P. Heue, G. Jaross, ML. Koukouli, E. Loots, R. Lutz, M.C Martinez Velarte, K. Michailidis, A. Pseftogkas, S. Nanda, S. Niemeijer, A. Pazmiño, G. Pinardi, A. Richter, N. Rozemeijer, M. Sneep, D. Stein Zweers, N. Theys, G. Tilstra, O. Torres, P. Valks, J. van Geffen, C. Vigouroux, P. Wang, and M. Weber.: S5P MPC Routine Operations Consolidated Validation Report series, Issue #27, Version 27.01.00, 227 pp., 15 June 2025.

Liang, R., Zhang, Y., Hu, Q., Li, T., Li, S., Yuan, W., Xu, J., Zhao, Y., Zhang, P., Chen, W., Zhuang, M., Shen, G., and Chen, Z.: Satellite-Based Monitoring of Methane Emissions from China's Rice Hub, Environmental Science & Technology, 58, 23127-23137, 10.1021/acs.est.4c09822, 2024.

Miller, S. M., Michalak, A. M., Detmers, R. G., Hasekamp, O. P., Bruhwiler, L. M. P., and Schwietzke, S.: China's coal mine methane regulations have not curbed growing emissions, Nature Communications, 10, 303, 10.1038/s41467-018-07891-7, 2019.

Murguia-Flores, F., Arndt, S., Ganesan, A. L., Murray-Tortarolo, G., and Hornibrook, E. R. C.: Soil Methanotrophy Model (MeMo v1.0): a process-based model to quantify global uptake of atmospheric methane by soil, Geosci. Model Dev., 11, 2009-2032, 10.5194/gmd-11-2009-2018, 2018.

Nassar, R., Hill, T. G., McLinden, C. A., Wunch, D., Jones, D. B. A., and Crisp, D.: Quantifying CO2 Emissions From Individual Power Plants From Space, Geophysical Research Letters, 44, 10,045-010,053, 10.1002/2017GL074702, 2017.

Saunois, M., Martinez, A., Poulter, B., Zhang, Z., Raymond, P. A., Regnier, P., Canadell, J. G., Jackson, R. B., Patra, P. K., Bousquet, P., Ciais, P., Dlugokencky, E. J., Lan, X., Allen, G. H., Bastviken, D., Beerling, D. J., Belikov, D. A., Blake, D. R., Castaldi, S., Crippa, M., Deemer, B. R., Dennison, F., Etiope, G., Gedney, N., Höglund-Isaksson, L., Holgerson, M. A., Hopcroft, P. O., Hugelius, G., Ito, A., Jain, A. K., Janardanan, R., Johnson, M. S., Kleinen, T., Krummel, P. B., Lauerwald, R., Li, T., Liu, X., McDonald, K. C., Melton, J. R., Mühle, J., Müller, J., Murguia-Flores, F., Niwa, Y., Noce, S., Pan, S., Parker, R. J., Peng, C., Ramonet, M., Riley, W. J., Rocher-Ros, G., Rosentreter, J. A., Sasakawa, M., Segers, A., Smith, S. J., Stanley, E. H., Thanwerdas, J., Tian, H., Tsuruta, A., Tubiello, F. N., Weber, T. S., van der Werf, G. R., Worthy, D. E. J., Xi, Y., Yoshida, Y., Zhang, W., Zheng, B., Zhu, Q., Zhu, Q., and Zhuang, Q.: Global Methane Budget 2000–2020, Earth Syst. Sci. Data, 17, 1873-1958, 10.5194/essd-17-1873-2025, 2025.

Zhang, Y., Fang, S., Chen, J., Lin, Y., Chen, Y., Liang, R., Jiang, K., Parker, R. J., Boesch, H., Steinbacher, M., Sheng, J.-X., Lu, X., Song, S., and Peng, S.: Observed changes in China's methane emissions linked to policy drivers, Proceedings of the National Academy of Sciences, 119, e2202742119, doi:10.1073/pnas.2202742119, 2022.